ACS APPLIED MATERIALS & INTERFACES

Research Article

www.acsami.org

Tailoring Graphene Nanosheets for Highly Improved Dispersion Stability and Quantitative Assessment in Nonaqueous Solvent

Minju Park,[†] Kyonghwa Song,[§] Taemin Lee,[†] JinHyeok Cha,[§] InWoong Lyo,[§] and Byeong-Su Kim*[,†,‡]

[†]Department of Energy Engineering and [‡]Department of Chemistry, Ulsan National Institute of Science and Technology (UNIST), Ulsan 44919, Korea

[§]Central Advanced Research & Engineering Institute, Hyundai Motor Company, Uiwang 16082, Korea

Supporting Information

ABSTRACT: Aggregation is a critical limitation for the practical application of graphene-based materials. Herein, we report that graphene oxide (GO) nanosheets chemically modified with ethanolamine (EA), ethylene glycol (EG), and sulfanilic acid (SA) demonstrate superior dispersion stability in organic solvents, specifically EG, based on the differences in their covalent chemistries. Functionalized GO was successfully dispersed in EG at a concentration of 9.0 mg mL^{-1} (0.50 vol %), the highest dispersion concentration reported to date. Moreover, our study introduces a unique analytical method for the assessment of dispersion stability and successfully quantifies the instability index based on transmission profiles under centrifugation cycles. Interestingly, GO-EG and GO-EA exhibited highly improved dispersion stabilities approximately 96 and 48 times greater than that of GO in EG solvent, respectively. This finding highlights the critical role of surface functional groups in the enhancement of chemical affinity and miscibility in the surrounding media. We anticipate that the novel structural designs and unique tools presented in this study will further the understanding and application of chemically functionalized carbon materials.

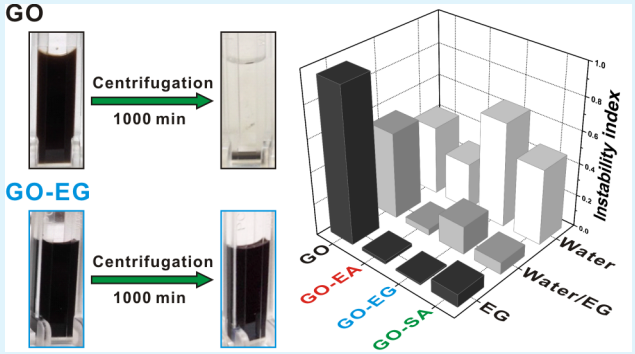

KEYWORDS: *graphene oxide, covalent functionalization, dispersion stability, quantitative assessment, ethylene glycol*

1. INTRODUCTION

While graphene has attracted significant interest due to its unique structure and outstanding properties, aggregation remains a critical obstacle for the large-scale application of pristine graphene.[1−4] To explore the unique features of graphene and further extend its practical application, chemically modified graphene, such as graphene oxide (GO) and reduced graphene oxide (rGO) suspensions, offers an attractive means of developing reliable and cost-effective synthetic methods for solution-processable graphene derivatives. GO is synthesized by the oxidative treatment of graphite, which yields oxidized graphene sheets decorated with hydroxyl and epoxide groups on the basal plane and carbonyl and carboxyl groups at the edge.[5] The presence of oxygen-containing functional groups renders GO strongly hydrophilic and provides excellent aqueous dispersity; however, aggregation is still observed at relatively high concentrations due to van der Waals interactions between the basal planes of the graphene nanosheets. Moreover, irreversible aggregation becomes more severe in organic solvents due to the disruption of hydrogen bonds between the oxygen functional groups and the solvent.[6] This phenomenon inhibits the solvent-philicity of GO and often poses technical difficulties for the fabrication of graphene-based materials and devices using organic solvents. Therefore, the large-scale production of graphene suspensions that are stable at high concentrations is important for practical applications.[7−11]

A number of approaches have been proposed to improve the dispersion stability of GO in both aqueous and organic media, including the addition of stabilizing molecules or surfactants on the surface of graphene, surface modification of the graphene sheet, and solvent exchange.[12−15] For example, Ruoff and coworkers reported a solvent exchange method to disperse rGO in organic solvents.[16] Furthermore, covalent functionalization of the surface of graphene has been suggested to improve its dispersion stability in various organic solvents.[6,15,17−19] Despite their widespread use, many approaches have only been implemented in relatively low concentration ranges (typically 0.1−1.0 mg mL^{-1}; maximum of 3.6 mg mL^{-1}; see Supporting Information, Table S1). Furthermore, analysis of the long-term suspension stability has been limited to either visual inspection or turbidity- and UV/vis-based optical characterization, which inevitably require diluted concentrations with unquantified stability values.

Herein, we present three different covalent functionalization approaches to improve the dispersion stability of GO

Received: June 15, 2016
Accepted: August 4, 2016
Published: August 4, 2016

DOI: 10.1021/acsami.6b07272
ACS Appl. Mater. Interfaces 2016, 8, 21595−21602

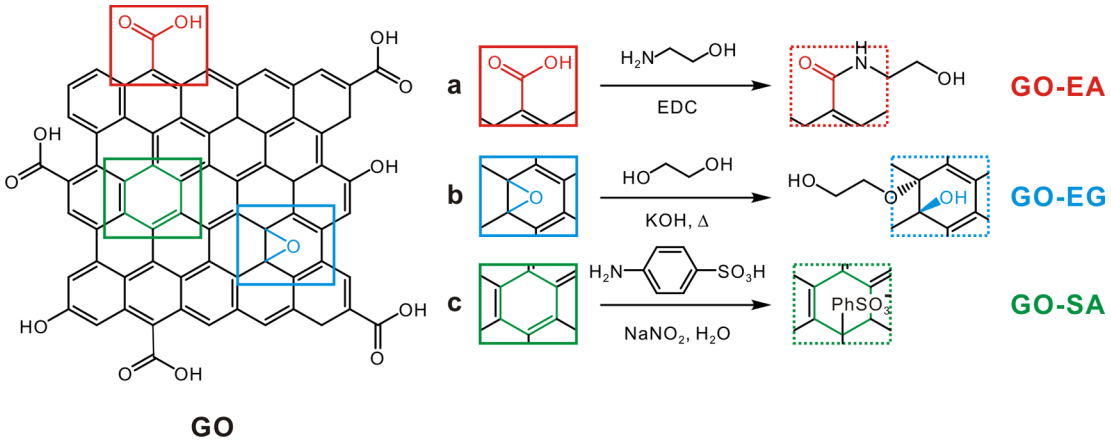

Figure 1. Schematic representation of the surface functionalization of GO nanosheets with (a) ethanolamine (EA), (b) ethylene glycol (EG), and (c) sulfanilic acid (SA) molecules to afford the respective functionalized GO-EA, GO-EG, and GO-SA nanosheets.

nanosheets in nonaqueous solvent. Among the many organic solvents, ethylene glycol (EG) was selected as the target testbed due to its miscibility with water and its widespread usage in antifreeze and coolants for heat transfer systems.[20−23] Moreover, when coupled with the outstanding thermal and mechanical properties of graphene-based structures, GO dispersion will open promising avenues for future nanofluids for thermal management applications.[20,24−26] Specifically, we introduced three types of molecules, including ethanolamine, ethylene glycol, and phenyl sulfonate groups, onto the GO nanosheets to demonstrate how the dispersion stability could be tailored by varying the functional molecules. Furthermore, another objective of this study was to provide an unequivocal assessment of the dispersion stability of functionalized GO nanosheets in both aqueous and nonaqueous solvents. The results reveal that the superior dispersion stability of functionalized GO nanosheets can be compared in a quantitative manner, which has been largely unexplored to date. We believe that this method provides a versatile strategy to achieve functionalized GO nanosheets with high dispersion stability in a desired solvent through the appropriate choice of functional group.

2. MATERIALS AND METHODS

2.1. Preparation of GO Suspensions and Covalent Surface Modification. Initially, graphite oxide powder was prepared by the oxidation of graphite (Sigma-Aldrich, <20 μm) using a modified Hummer's method and exfoliated to give a brown dispersion of graphene oxide (GO) under ultrasonication (typical concentration of 1.00 mg mL^{-1}). For the chemical functionalization of the carboxylic acid groups of GO with ethanolamine (GO-EA), 50 mL of the pristine GO suspension was reacted with 10 mL of EA in the presence of 1.0 g *N*-ethyl-*N*′-(3-dimethyl aminopropyl)carbodiimide methiodide (EDC) for 12 h at room temperature, followed by extensive dialysis (SpectraPore MWCO 12−14 K) for 4 days to remove any byproducts and remaining reactants. Ethylene glycol-functionalized GO (GO-EG) was synthesized by the reaction of the epoxy group of GO and EG. 5.0 mL of EG was mixed with 0.3 g of potassium hydroxide at 50 °C for 1 h, and the mixture was added to 50 mL of GO suspension. After the reaction, the purification steps were identical to the process for GO-EA. Sulfonate graphene oxide (GO-SA) was synthesized through an aryl diazonium reaction of sulfanilic acid. The aryl diazonium salt was prepared from the reaction of 460 mg of sulfanilic acid and 200 mg of sodium nitrite in 100 mL of water (the mixture turned yellow as the reaction proceeded). After 7.0 mL of 1.0 M HCl solution was added to this mixture in an ice bath under stirring, the yellow color of the reaction mixture disappeared, and the dispersion was stored in the ice bath for over 2 h.[27,28] After the reaction, the purification steps were identical to the process for GO-EA.

2.2. Stability Test. The stability of the functionalized GO dispersions was investigated by observing the sedimentation behavior under centrifugation at 4000 rpm (2300*g*) using a LUMiFuge LF 111 instrument (L.U.M. GmbH, Berlin, Germany). Initially, the functionalized GO suspensions were freeze-dried to remove water and then redispersed in water and EG at a concentration of 9.0 mg mL^{-1} by ultrasonication. The dispersions were transferred to measuring tubes, and an optoelectronic sensor system enabled the spatial and temporal changes in the light transmission to be monitored during centrifugation. The temperature was held constant at 25 °C, and the local transmission was determined over the entire sample. Thus, the instability index and the velocity of the sedimentation were investigated simultaneously based on the transmission profiles of the samples. The red lines represent the transmission profiles in the early stages, and the green lines correspond to later stages. It was possible to describe the separation process based on the time and relative position under centrifugation and to trace the overall separation processes.[29]

2.3. Characterization. The ζ-potential of the colloidal suspensions was measured using a ζ-potential analyzer (Malvern, Zetasizer nanozs). The elemental analyzer (Flash 2000) was used to determine the relative atomic composition, which was used to determine the structure of the unknown compound after the chemical modification of GO. FT-IR spectroscopy was used to determine the chemical structure and bonding of the functionalized GO materials with ATR-mode (Varian 670). The surface morphologies of the GO and functionalized GO were examined using an atomic force microscope (AFM, Dimension D3100, Veeco). The average thickness was calculated by choosing 30 random points, and the average area was calculated by a SemAfore 5.21 program with 20 random nanosheets. X-ray photoelectron spectroscopy (XPS, Thermo Fisher, K-alpha) was used to detect the elemental composition and the chemical state of the functionalized GO dispersions. The stability of the dispersions was investigated using a LUMiFuge LF 111 instrument (L.U.M. GmbH, Berlin, Germany). The concentrations of impurities were quantified using inductively coupled plasma optical emission spectroscopy (ICP-OES, 700-ES, Varian) in triplicate, and the average value was used in this study. The rheological behavior was determined using a Haake MARS III instrument, which measures viscosity as a function of shear rate. The temperature was maintained at room temperature.

3. RESULTS AND DISCUSSION

3.1. Preparation of GO−Derivatives through Covalent Functionalization. The GO nanosheet was prepared by the oxidation of graphite according to a modified Hummers' method.[30] The chemical functional groups introduced on the surface of the graphene nanosheet, including carboxylic acids,

DOI: 10.1021/acsami.6b07272
ACS Appl. Mater. Interfaces 2016, 8, 21595−21602

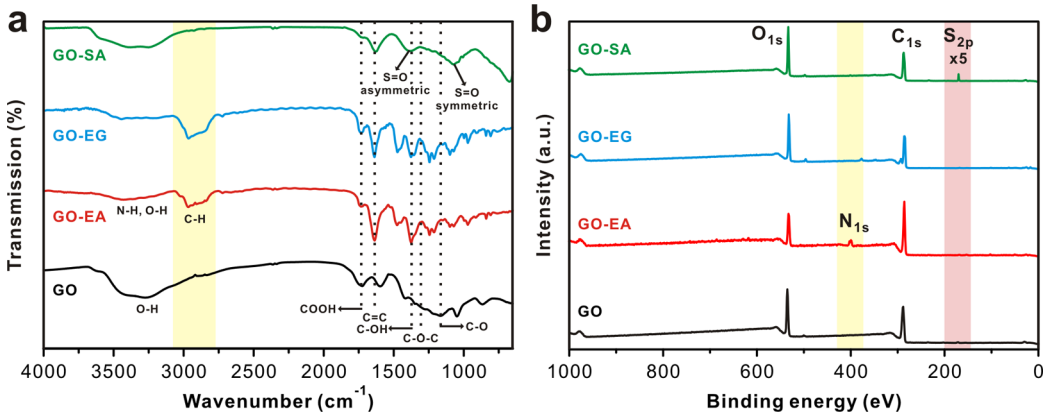

Figure 2. (a) FT-IR spectra and (b) XPS survey spectra of GO, GO-EA, GO-EG, and GO-SA.

phenolic alcohols, and epoxy groups, rendered the GO suspension negatively charged over a wide range of pH conditions (ζ-potential of −40 mV).[31] In the initial stage of our work, we prepared a series of GO nanosheets chemically functionalized with three different molecules as follows: ethanolamine (EA), ethylene glycol (EG), and sulfanilic acid (SA) (Figure 1). These molecules were introduced to enhance the dispersion stability of graphene nanosheets in the target solvent based on the differences in their covalent chemistries.

First, *N*-ethyl-*N*′-(3-(dimethylamino)propyl)carbodiimide methiodide (EDC)-mediated surface functionalization of GO was achieved through the reaction of carboxylic acids and the amine groups of EA, and the product is denoted hereafter as GO-EA. In our previous studies, identical methods have been successfully integrated to introduce various amine functional molecules onto the surface of GO.[32−34] Because the carboxylic acid groups are mostly located at the edge, functionalized EA was predominantly attached at the edge of the graphene nanosheets. Second, graphene oxide functionalized with EG (GO-EG) was synthesized through the reaction of epoxy groups and hydroxyl groups under basic conditions. Epoxy groups decorate on the basal plane of the GO nanosheets; therefore, functionalization mainly occurred on the surface of the graphene nanosheets. We postulate that EG-like molecules, such as EA and EG, would improve the dispersion stability in EG solvent due to the similarity of their molecular structures. Furthermore, we demonstrated how the dispersion stability could be enhanced by varying the location of the functional groups. Finally, sulfonated graphene oxide (GO-SA) was prepared by directly anchoring sulfonic acid-containing aryl radicals to the surface of graphene sheets via diazonium chemistry.[27,35] The phenylsulfonic acid group has a very low pK_a (−6.62),[36] and this negative charge of the sulfonate group induces a significant repulsive force between the graphene nanosheets. For this reason, the highly charged sulfonate groups of GO-SA may prevent the graphitic sheets from aggregating and thereby improve their water solubility. By synthesizing these three different GOs, we demonstrate how the dispersion stability can be enhanced by varying the location and chemical structure of the functionalized molecules.

3.2. Characterization of GO−Derivatives. The successful functionalization of each molecule on the GO nanosheet was confirmed by FT-IR and X-ray photoelectron spectroscopy (XPS) (Figure 2). The FT-IR spectra revealed that the pristine GO displayed three characteristic peaks at 3200−3500, 1725, and 1315 cm^{-1} corresponding to the hydroxyl (OH), carboxylic acid (COOH), and epoxy (C−O−C) groups, respectively.[37−39] The functionalized GO-EA and GO-EG exhibited two additional peaks at 2966 and 2865 cm^{-1}, indicating asymmetric and symmetric stretching modes of C−H bonds from ethylene spacer group in ethanolamine and ethylene glycol, respectively.[40] The peak intensity of the carboxylic acid was considerably lower after the functionalization of GO-EA, leading to the formation of an amide bond with EA at around 1640 cm^{-1}. Since the location of a peak with conjugated C=C bond, and amide bond was overlapped, it was hard to deconvolute; however, the overall peak intensity was clearly increased. A decrease in the epoxy band was also observed in both GO-EA and GO-EG, which indicates that the ring-opening reaction of epoxides was inevitable with excess amine and alkoxide groups. In a separate reaction of GO-SA, peaks were observed at 1382 and 1072 cm^{-1}, corresponding to respective asymmetric and symmetric S=O stretching, confirming the presence of the sulfonic acid group.[27] In order to further analyze the atomic composition of the functionalized GO nanosheets, XPS and elemental analysis were performed. As shown in Figure 2b, we found a distinct evolution of nitrogen peak in GO-EA (approximately 6.7 at. %), while negligible nitrogen content was detected in GO, GO-EG, and GO-SA. In accordance with the XPS analysis, elemental analysis data confirmed the successful introduction of the functional groups onto the GO nanosheet (Table 1). For example, nitrogen was only detected in GO-EA, indicating the functionalization of amine groups onto the GO. Moreover, the sulfonate group of GO-SA was introduced on the surface of the GO nanosheet up to 1.0% after the anchoring of the sulfonic acid groups.

Table 1. Relative Atomic Composition Based on XPS and Elemental Analysis Measurements

	atomic ratio measured by XPS				weight ratio measured by elemental analysis			
compd	C 1s	O 1s	N 1s	S 2p	C	O	N	S
GO	71.1	27.4	ND[a]	0.7[b]	48.5	45.7	ND	1.0[b]
GO-EA	73.4	18.6	6.7	ND	52.6	29.6	9.8	ND
GO-EG	69.6	26.1	ND	ND	47.7	42.0	ND	ND
GO-SA	66.7	30.9	0.6	1.0	48.2	44.5	ND	0.94

[a]Values below the detection limit of the XPS and elemental analysis are represented as not detectable (ND). [b]A trace amount of sulfur originated from the sulfuric acid in the synthesis of GO.

DOI: 10.1021/acsami.6b07272
ACS Appl. Mater. Interfaces 2016, 8, 21595−21602

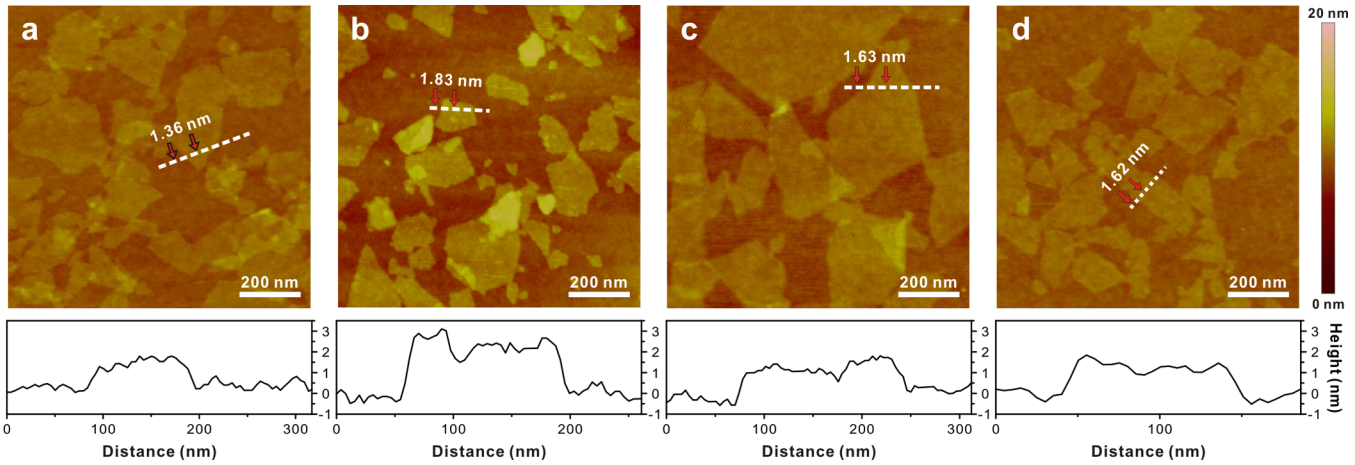

Figure 3. Representative AFM images of (a) GO, (b) GO-EA, (c) GO-EG, and (d) GO-SA with the corresponding line scan profiles. All GO samples were deposited on a silicon wafer from an aqueous dispersion.

The complete removal of metal salts, which often remain in graphite oxide, is another critical issue to dispersion stability of fabricated GO. These residual impurities could neutralize the charge of GO, thereby increasing aggregation and destabilization.[2] In addition to the contaminating materials originating from the chemical reagents used during synthesis, metal impurities not associated with the synthetic process were also observed. According to previous research, the main ion impurities in GO are Mn, Fe, and K.[41] As a result of the extensive purification cycles that we employed, our GO and its derivatives retained metallic impurities at the level of several ppm, as measured by inductively coupled plasma optical emission spectroscopy (ICP-OES). These levels are much lower than those reported in other studies (see Supporting Information, Table S2).[41−43] Thus, we confirmed that the observed dispersion stability is mainly due to the presence of functional groups on the surface of the GO nanosheets.

Atomic force microscopy (AFM) images demonstrated that the prepared GO nanosheets were mainly composed of a monolayer of graphene nanosheets with an average thickness of 1.39 ± 0.14 nm and an area of 0.039 ± 0.010 μm^2 (Figure 3a and Figure S1). It should be noted that the single-layer GO nanosheet was significantly thicker than the pristine graphene due to the presence of oxygen functional groups, atomic-scale roughness arising from structural defects, and adsorbed solvent molecules, in agreement with previous studies.[2,7,44,45] After chemical modification, the thicknesses of GO-EA (1.97 ± 0.19 nm), GO-EG (1.65 ± 0.16 nm), and GO-SA (1.57 ± 0.20 nm), which were averaged over 30 samples, were greater than that of GO (1.39 ± 0.14 nm) (Figure 3b−d). In addition, there were slight changes in the area of the graphene nanosheets in GO derivatives, GO-EA (0.025 ± 0.013 μm^2), GO-EG (0.053 ± 0.023 μm^2), and GO-SA (0.036 ± 0.018 μm^2), reflecting the fact that the mild nature of this synthetic approach does not alter the intrinsic properties of the graphene nanosheet.

Further investigation of the structural changes during functionalization was also conducted by Raman spectral analysis (see Figure S2 in the Supporting Information). GO displayed two prominent peaks at 1334 and 1604 cm^{-1}, which correspond to the symmetry A_{1g} mode of the D band and the E_{2g} mode of the sp^2 carbon atoms of the G band, respectively.[44,46] It is well established that the D band corresponds to structural defects, an amorphous structure, or edges that break the symmetry, while the G band is associated with graphitic sp^2 carbon domains.[47] The strong intensity of the D band indicated a high density of defects and the presence of edge functional groups in GO and covalently functionalized GO. Neither the D nor the G peak positions changed after the functionalization, and the peak intensity ratio of I_D/I_G remained almost constant (1.12−1.21), implying that the structure of the carbon domain was maintained during chemical functionalization. Taken together, we argue that the dispersibility of the functionalized GO derivatives was mainly influenced by the different covalent chemistries that introduced the various functional groups onto the surface of the GO nanosheets.

3.3. Quantitative Assessment for the Dispersion Stability. To obtain detailed quantitative information about the dispersion stability, we utilized a new method based on measuring sedimentation behavior under a high centrifugation force. The separation analysis of the functionalized GO materials was performed by a LUMiFuge system, which determines the space- and time-resolved extinction profiles between the bottom and the fluid level during centrifugation (Figure 4). Using centrifugation force enables the acceleration of the sedimentation of particles, leading to clarification of the dispersion. NIR transmission profiles were measured in situ every minute under centrifugation at 4000 rpm (2300g) at room temperature.[38] Several reports have utilized this method

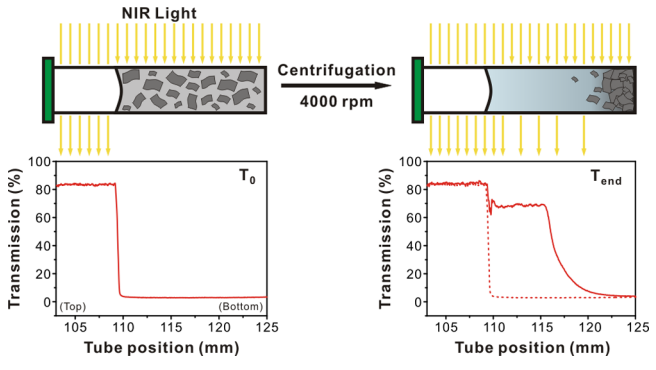

Figure 4. Schematic representation and the corresponding transmission profile for the analysis of the dispersion stability of covalent functionalized GO suspensions using transmission profiles under centrifugation system. The transmission of near-infrared (NIR) irradiation was measured over the entire sample tube to allow spatial and temporal changes of GO dispersion during centrifugation.

DOI: 10.1021/acsami.6b07272
ACS Appl. Mater. Interfaces 2016, 8, 21595−21602

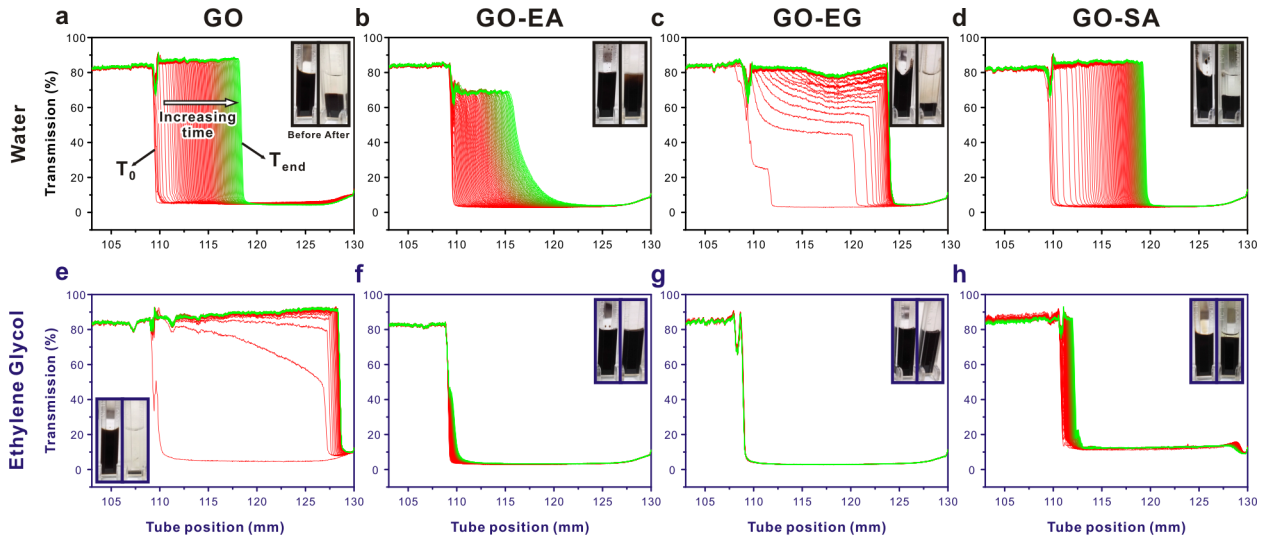

Figure 5. Transmission profiles of functionalized GO suspensions in different solvents: water (top panel) and ethylene glycol (bottom panel). (a,e) GO, (b,f) GO-EA, (c,g) GO-EG, and (d,h) GO-SA. The red line represents the first scan and the green line the last scan (t = 1000 min), with a regular scan reported every 10 min at a concentration of 9.0 mg mL^{-1} using a LUMiFuge instrument under 4000 rpm (2300g) at room temperature. The inset images display the respective suspension (left) before and (right) after centrifugation.

to analyze the sedimentation behavior of carbon-based materials;[38,48,49] however, only a few studies have reported the sedimentation behavior of graphene-based materials.[50,51] As mentioned earlier, while the assessment of the dispersion stability of GO has suffered as a result of the limitations of traditional approaches, which rely on the visual- or UV/vis spectroscopy-based inspection of a diluted suspension for a relatively long time period (several weeks or even years), this new investigation presents the following advantages: (1) the dispersion stability can be quantified by calculating the instability index and sedimentation velocity; (2) a highly concentrated (9.0 mg mL^{-1}) suspension was quantified, corresponding to the highest concentration reported to date; (3) the time scale for the measurement was effectively reduced by using high-speed centrifugation; and (4) the sedimentation behavior and size distribution could be explored at the same time as the dispersion stability.

In the case of a stable suspension, the interval between each transmission profile is small due to slow sedimentation. However, fast sedimentation, which is indicative of an unstable suspension, causes a considerable change in transmission over a short time. Furthermore, each particle settles independently according to its size; thus, a broad size distribution leads to horizontal changes in the transmission.

All functionalized GO derivatives were dispersed in water (top panel in Figure 5) and EG (bottom panel in Figure 5) at a concentration of 9.0 mg mL^{-1}, which is considerably higher than the typical working concentration ranges (below 1.0 mg mL^{-1}). The initial transmission value at t = 0 was not related to the stability of the dispersion. However, the change in transmission over time is directly related to the dispersion stability and sedimentation velocity. The profiles of unmodified GO in water gradually shifted to the right, which suggests that sedimentation occurred under centrifugation (Figure 5a). In accordance with the sedimentation profile curve, the inset image clearly indicated the precipitation of unstable graphene nanosheets during measurement. In addition, it is worth noting that the vertical slope in the transmission profiles suggested that the GO dispersion was composed of uniformly sized nanosheets possessing an identical sedimentation velocity throughout the measurements. In contrast, the GO-EA suspension in water displayed slightly slanted transmission profiles (Figure 5b). This observation indicates that there was a size distribution in the suspension. The existing size distribution of GO-EA could originate from the reactivity of EA, which may react with the carboxylic acid group at the edges of the graphene nanosheets as well as the epoxide groups on the basal plane, eventually producing a bond bridging the two layers of graphene.[52] In accordance with the aforementioned observation, it was also interesting to note that the GO-EA showed more stacked layers with a relatively broad size distribution in the AFM images (Figure 3b). In Figure 5c, the GO-EG nanosheets were relatively unstable under extensive centrifugation compared with that of other GO derivatives. According to recent studies, pristine GO is composed of functionalized graphene sheets decorated with strongly bound oxidative debris, which acts as a surfactant to stabilize aqueous GO suspensions.[53,54] These oxidative debris are strongly adhered to the surface of GO in acidic or neutral conditions; however, it becomes separated under basic conditions due to the negative charge of the deprotonated debris. As a result, the dispersion stability of GO-EG in water was slightly decreased. GO-SA represented a similar profile to the GO solution (Figure 5d). Although the highly charged SO^{3-} groups of GO-SA were expected to prevent aggregation and improve dispersion stability in water, the repulsive force between the negative charges was too weak to overcome the centrifugation force and the interactions between the graphene sheets at high concentrations.

We then further investigated the suspension stability of functionalized GO derivatives in EG solvent. Initially, the GO nanosheets precipitated within 30 min in pure EG, which indicated highly unstable behavior (Figure 5e). In contrast to the previous report of Paredes et al. in which they observed a stable dispersion of GO in EG solvent for 3 weeks at a concentration 0.5 mg mL^{-1},[45] we found that the GO suspension eventually became unstable at higher concentrations in EG. This observation highlights the critical advantage of the

DOI: 10.1021/acsami.6b07272
ACS Appl. Mater. Interfaces 2016, 8, 21595−21602

current approach over other conventional techniques. In contrast, GO-EA and GO-EG, which were functionalized with EG-like molecules, demonstrated negligible changes in their transmission profiles during the measurement (Figure 5f and g). In particular, GO-EG showed virtually no change in its transmission profile, and sedimentation did not occur after 1000 min, even under excessive centrifugation cycles at high gravity force (2300*g*). The closely packed lines implied that the GO-EG suspension possessed a superior solubility and stability in EG solvent. This result highlights the importance of establishing an intimate interface between the solvent (EG) and graphene derivatives (GO-EA and GO-EG) to retain excellent dispersion stability owing to their structural similarity. In addition, GO-SA showed better dispersion stability in EG than did GO. Because of the bulky functional group on the graphene surface, the aggregation of the nanosheets in EG solvent might be prevented by the steric hindrance between them (Figure 5h). Additional information about transmission profiles in the water/EG mixture and sedimentation velocity are included in Supporting Information (Figure S3 and Table S3).

3.4. Dispersion Stability in Other Nonaqueous Solvents. According to recent literatures, GO itself could be dispersed well in several nonaqueous solvents including DMF and NMP, which exhibited a long-term stability for more than 3 weeks.[45] As a representative example of our functionalized GO, GO-EG was dispersed in both DMF and NMP (Figure S4). It was dispersed well in both media at a concentration of 1.0 mg mL^{-1}. However, upon centrifugation under high centrifugal force (4000 rpm), the GO-EG started to precipitate within 30 min, suggesting the relative unstable behavior of GO-EG in both solvents for a long period. Once again, this result clearly revealed the critical role of surface functional groups for achieving the optimum stability of dispersion in a desired solvent.

3.5. Rheological Behaviors of GO-Based Dispersions. During fabrication, a significant viscosity change was observed in GO and the functionalized GO samples at high concentrations. Because of the friction force between graphene sheets, high viscosity could affect the suspension stability. To clarify this effect, the viscosity of each GO suspension at high concentration was measured to investigate its rheological properties (Figure S5, Supporting Information). The viscosities of all GO and functionalized GO materials increased due to the high concentration. In particular, the viscosities of GO-SA and GO-EG in EG solvent were much higher than the base fluid of viscosities of approximately 39.18 and 35.00 mPa·s, respectively. However, the viscosity of GO-EA remained almost unchanged in all solvents. Because high viscosity could prevent the precipitation of nanosheets in suspension, a diluted GO suspension (0.50 mg mL^{-1}) was prepared in water/EG solvent, and both the viscosity and dispersion stability were measured (Figure S6). While the viscosity was similar to the base fluid at approximately 3.70 mPa·s, the dispersion stability improved compared with concentrated suspensions. Therefore, we concluded that suspensions of the functionalized GO diluted to within a conventional concentration range (below 1.0 mg mL^{-1}) would possess much better dispersion stabilities than the concentrated functionalized GO prepared herein.

3.6. Instability Index. Although the individual line of transmission does not correspond to the dispersion stability or sedimentation velocity, the difference in integral transmission versus time is directly related to the dispersion stability. We have extracted the instability index, a quantifiable parameter based on the transmission profiles as defined below (ISO/TR 13097:2013 Guidelines for the characterization of dispersion stability):

$$\text{Instability index} = \frac{\Delta T_i}{\Delta T_{\max}} = \frac{\sum_{j=r_{\min}}^{r_{\max}} T_{i,j}^{diff}}{(\overline{T}_{End} - \overline{T}_1)\cdot(r_{\max} - r_{\min})}$$

where T^{diff} represents the difference between the first and subsequent transmission ($T_i - T_1$), r is the range of the sample analyzed, and j is the respective number of the position increment. The instability index is calculated from the normalization of the change in transmission with the highest transmission $\overline{T}_{end}$ achieved and is reported as a dimensionless number between 0 and 1. Zero represents no change in the transmission profile (very stable suspension), while an instability index of one indicates a completely separated suspension with very low stability.

The instability index was extracted from transmission measurements for all the GO dispersions (Figure 6 and Table 2). In water, all of the suspensions displayed a moderate dispersion stability of between 0.29 and 0.65. As EG was added to water (water/EG mixture), the instability index increased in the GO suspension, whereas the covalently functionalized GO

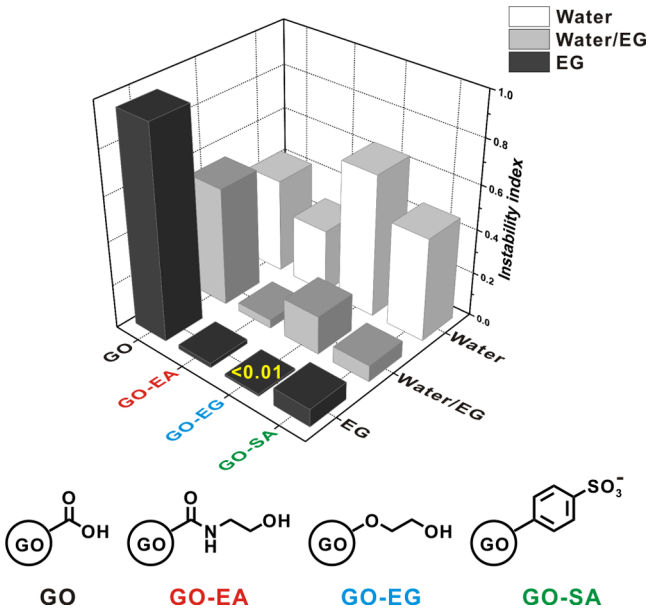

Figure 6. 3D matrix of the instability index of functionalized GO in different solvents: water, water/EG (1:1), and EG with a corresponding schematic representation of the covalently functionalized GO samples. The instability index was calculated on the basis of the sedimentation transmission curves shown in Figure 5 and Figure S3.

Table 2. Instability Indices in Different Solvents Calculated from the Transmission Profile

	instability index		
compound	water	water/EG	EG
GO	0.430	0.539	0.958
GO-EA	0.293	0.039	0.02
GO-EG	0.648	0.175	< 0.01
GO-SA	0.469	0.074	0.08

DOI: 10.1021/acsami.6b07272
ACS Appl. Mater. Interfaces 2016, 8, 21595−21602

dispersions all exhibited lower values. Moreover, in pure EG solvent, the instability indices of GO and covalently modified GO dispersions were considerably different. The instability index of GO was 0.96, and the suspension was highly unstable, rapidly precipitating as soon as centrifugation was initiated. However, functionalized GO, especially GO-EA and GO-EG, showed significantly lower instability index values in EG solvent. Specifically, in the EG solvent, the GO-EG and GO-EA suspensions were approximately 96 and 48 times more stable than GO. These findings show that the dispersion stability can be tailored by varying the functional groups on functionalized GO to achieved a desirable stability in a given solvent.

4. CONCLUSIONS

In summary, we have developed a facile approach for the surface modification of GO nanosheets to enhance the dispersion stability in the organic solvent EG. FT-IR, XPS, AFM, elemental analysis, and Raman measurements confirm the successful covalent functionalization of GO-EA, GO-EG, and GO-SA without significant morphological changes of the nanosheets. As a result, the structural similarities resulted in a highly improved affinity between the functionalized GO materials and EG solvent; thus, excellent dispersion stability was maintained at high concentrations up to 9.0 mg mL^{-1}. The other meaningful aspect of this research was that the dispersion stability of GO and its derivatives could be quantified by the instability index and sedimentation velocity, which have been largely unexplored to date. Although the current conclusion is applicable in GO derivatives with relatively small lateral dimension, it affords versatile opportunities to achieve a highly stable dispersion in a desired solvent, which increases the viability of a large-scale technological application of GO in organic solvents. The stable graphene based suspension in EG will provide promising ways for the fabrication of heat transfer systems such as coolants or antifreeze applications.

■ ASSOCIATED CONTENT

Supporting Information

The Supporting Information is available free of charge on the ACS Publications website at DOI: 10.1021/acsami.6b07272.

Additional ICP-OES, Raman, rheological analysis, and transmission profiles (PDF)

■ AUTHOR INFORMATION

Corresponding Author

*E-mail: bskim19@unist.ac.kr.

Author Contributions

M.P., K.S., and B.-S.K. designed the research. M.P. performed all experiments. M.P., T.L., and B.-S.K. contributed to analysis and wrote the manuscript and supporting text. All authors discussed and commented on the manuscript.

Notes

The authors declare no competing financial interest.

■ ACKNOWLEDGMENTS

This work was supported by the National Research Foundation of Korea (NRF) (NRF-2014R1A2A1A11052829) and the Hyundai Motor Company (2.150078.01). M.P. acknowledges financial support from the Global Ph.D. Fellowship (GPF) funded by the National Research Foundation of Korea (NRF) (NRF-2014H1A2A1018269).

■ REFERENCES

(1) Geim, A. K.; Novoselov, K. S. The Rise of Graphene. *Nat. Mater.* **2007**, *6*, 183−191.

(2) Li, D.; Muller, M. B.; Gilje, S.; Kaner, R. B.; Wallace, G. G. Processable Aqueous Dispersions of Graphene Nanosheets. *Nat. Nanotechnol.* **2008**, *3*, 101−105.

(3) Sun, Y.; Wu, Q.; Shi, G. Graphene Based New Energy Materials. *Energy Environ. Sci.* **2011**, *4*, 1113−1132.

(4) Nair, R. R.; Blake, P.; Grigorenko, A. N.; Novoselov, K. S.; Booth, T. J.; Stauber, T.; Peres, N. M. R.; Geim, A. K. Fine Structure Constant Defines Visual Transparency of Graphene. *Science* **2008**, *320*, 1308−1308.

(5) Stankovich, S.; Dikin, D. A.; Piner, R. D.; Kohlhaas, K. A.; Kleinhammes, A.; Jia, Y.; Wu, Y.; Nguyen, S. T.; Ruoff, R. S. Synthesis of Graphene-Based Nanosheets Via Chemical Reduction of Exfoliated Graphite Oxide. *Carbon* **2007**, *45*, 1558−1565.

(6) Stankovich, S.; Piner, R. D.; Nguyen, S. T.; Ruoff, R. S. Synthesis and Exfoliation of Isocyanate-Treated Graphene Oxide Nanoplatelets. *Carbon* **2006**, *44*, 3342−3347.

(7) Stankovich, S.; Dikin, D. A.; Dommett, G. H. B.; Kohlhaas, K. M.; Zimney, E. J.; Stach, E. A.; Piner, R. D.; Nguyen, S. T.; Ruoff, R. S. Graphene-Based Composite Materials. *Nature* **2006**, *442*, 282−286.

(8) Zhang, K.; Mao, L.; Zhang, L. L.; On Chan, H. S.; Zhao, X. S.; Wu, J. Surfactant-Intercalated, Chemically Reduced Graphene Oxide for High Performance Supercapacitor Electrodes. *J. Mater. Chem.* **2011**, *21*, 7302−7307.

(9) Lotya, M.; Hernandez, Y.; King, P. J.; Smith, R. J.; Nicolosi, V.; Karlsson, L. S.; Blighe, F. M.; De, S.; Wang, Z.; McGovern, I. T.; Duesberg, G. S.; Coleman, J. N. Liquid Phase Production of Graphene by Exfoliation of Graphite in Surfactant/Water Solutions. *J. Am. Chem. Soc.* **2009**, *131*, 3611−3620.

(10) Stankovich, S.; Piner, R. D.; Chen, X.; Wu, N.; Nguyen, S. T.; Ruoff, R. S. Stable Aqueous Dispersions of Graphitic Nanoplatelets Via the Reduction of Exfoliated Graphite Oxide in the Presence of Poly(Sodium 4-Styrenesulfonate). *J. Mater. Chem.* **2006**, *16*, 155−158.

(11) Lin, Y.; Gao, L.; Sun, J.; Wang, Y.; Zhang, J. Stable Nafion-Functionalized Graphene Dispersions for Transparent Conducting Films. *Nanotechnology* **2009**, *20*, 465605.

(12) Xu, Y.; Bai, H.; Lu, G.; Li, C.; Shi, G. Flexible Graphene Films Via the Filtration of Water-Soluble Noncovalent Functionalized Graphene Sheets. *J. Am. Chem. Soc.* **2008**, *130*, 5856−5857.

(13) Cai, X.; Tan, S.; Lin, M.; Xie, A.; Mai, W.; Zhang, X.; Lin, Z.; Wu, T.; Liu, Y. Synergistic Antibacterial Brilliant Blue/Reduced Graphene Oxide/Quaternary Phosphonium Salt Composite with Excellent Water Solubility and Specific Targeting Capability. *Langmuir* **2011**, *27*, 7828−7835.

(14) Zhuang, X.-D.; Chen, Y.; Liu, G.; Li, P.-P.; Zhu, C.-X.; Kang, E.-T.; Noeh, K.-G.; Zhang, B.; Zhu, J.-H.; Li, Y.-X. Conjugated-Polymer-Functionalized Graphene Oxide: Synthesis and Nonvolatile Rewritable Memory Effect. *Adv. Mater.* **2010**, *22*, 1731−1735.

(15) Tessonnier, J.-P.; Barteau, M. A. Dispersion of Alkyl-Chain-Functionalized Reduced Graphene Oxide Sheets in Nonpolar Solvents. *Langmuir* **2012**, *28*, 6691−6697.

(16) Park, S.; An, J.; Jung, I.; Piner, R. D.; An, S. J.; Li, X.; Velamakanni, A.; Ruoff, R. S. Colloidal Suspensions of Highly Reduced Graphene Oxide in a Wide Variety of Organic Solvents. *Nano Lett.* **2009**, *9*, 1593−1597.

(17) Qi, X.; Pu, K.-Y.; Zhou, X.; Li, H.; Liu, B.; Boey, F.; Huang, W.; Zhang, H. Conjugated-Polyelectrolyte-Functionalized Reduced Graphene Oxide with Excellent Solubility and Stability in Polar Solvents. *Small* **2010**, *6*, 663−669.

(18) Zhong, Z.; Dai, Y.; Ma, D.; Wang, Z. Y. Facile Synthesis of Organo-Soluble Surface-Grafted All-Single-Layer Graphene Oxide as Hole-Injecting Buffer Material in Organic Light-Emitting Diodes. *J. Mater. Chem.* **2011**, *21*, 6040−6045.

(19) Choudhary, S.; Mungse, H. P.; Khatri, O. P. Dispersion of Alkylated Graphene in Organic Solvents and Its Potential for Lubrication Applications. *J. Mater. Chem.* **2012**, *22*, 21032−21039.

DOI: 10.1021/acsami.6b07272
ACS Appl. Mater. Interfaces 2016, 8, 21595−21602

(20) Kole, M.; Dey, T. K. Investigation of Thermal Conductivity, Viscosity, and Electrical Conductivity of Graphene Based Nanofluids. *J. Appl. Phys.* **2013**, *113*, 084307.
(21) Eastman, J. A.; Choi, S. U. S.; Li, S.; Yu, W.; Thompson, L. J. Anomalously Increased Effective Thermal Conductivities of Ethylene Glycol-Based Nanofluids Containing Copper Nanoparticles. *Appl. Phys. Lett.* **2001**, *78*, 718−720.
(22) Jha, N.; Ramaprabhu, S. Thermal Conductivity Studies of Metal Dispersed Multiwalled Carbon Nanotubes in Water and Ethylene Glycol Based Nanofluids. *J. Appl. Phys.* **2009**, *106*, 084317.
(23) Garg, J.; Poudel, B.; Chiesa, M.; Gordon, J. B.; Ma, J. J.; Wang, J. B.; Ren, Z. F.; Kang, Y. T.; Ohtani, H.; Nanda, J.; McKinley, G. H.; Chen, G. Enhanced Thermal Conductivity and Viscosity of Copper Nanoparticles in Ethylene Glycol Nanofluid. *J. Appl. Phys.* **2008**, *103*, 074301.
(24) Hadadian, M.; Goharshadi, E. K.; Youssefi, A. Electrical Conductivity, Thermal Conductivity, and Rheological Properties of Graphene Oxide-Based Nanofluids. *J. Nanopart. Res.* **2014**, *16*, 1−17.
(25) Yu, W.; Xie, H.; Wang, X.; Wang, X. Significant Thermal Conductivity Enhancement for Nanofluids Containing Graphene Nanosheets. *Phys. Lett. A* **2011**, *375*, 1323−1328.
(26) Sen Gupta, S.; Manoj Siva, V.; Krishnan, S.; Sreeprasad, T. S.; Singh, P. K.; Pradeep, T.; Das, S. K. Thermal Conductivity Enhancement of Nanofluids Containing Graphene Nanosheets. *J. Appl. Phys.* **2011**, *110*, 084302.
(27) Si, Y.; Samulski, E. T. Synthesis of Water Soluble Graphene. *Nano Lett.* **2008**, *8*, 1679−1682.
(28) Ji, J.; Zhang, G.; Chen, H.; Wang, S.; Zhang, G.; Zhang, F.; Fan, X. Sulfonated Graphene as Water-Tolerant Solid Acid Catalyst. *Chem. Sci.* **2011**, *2*, 484−487.
(29) Beckert, F.; Rostas, A. M.; Thomann, R.; Weber, S.; Schleicher, E.; Friedrich, C.; Mülhaupt, R. Self-Initiated Free Radical Grafting of Styrene Homo- and Copolymers onto Functionalized Graphene. *Macromolecules* **2013**, *46*, 5488−5496.
(30) Hummers, W. S.; Offeman, R. E. Preparation of Graphitic Oxide. *J. Am. Chem. Soc.* **1958**, *80*, 1339−1339.
(31) Lee, D. W.; Hong, T.-K.; Kang, D.; Lee, J.; Heo, M.; Kim, J. Y.; Kim, B.-S.; Shin, H. S. Highly Controllable Transparent and Conducting Thin Films Using Layer-by-Layer Assembly of Oppositely Charged Reduced Graphene Oxides. *J. Mater. Chem.* **2011**, *21*, 3438−3442.
(32) Park, M.; Lee, T.; Kim, B.-S. Covalent Functionalization Based Heteroatom Doped Graphene Nanosheet as a Metal-Free Electrocatalyst for Oxygen Reduction Reaction. *Nanoscale* **2013**, *5*, 12255−12260.
(33) Jeon, E. K.; Seo, E.; Lee, E.; Lee, W.; Um, M.-K.; Kim, B.-S. Mussel-Inspired Green Synthesis of Silver Nanoparticles on Graphene Oxide Nanosheets for Enhanced Catalytic Applications. *Chem. Commun.* **2013**, *49*, 3392−3394.
(34) Hwang, H.; Joo, P.; Kang, M. S.; Ahn, G.; Han, J. T.; Kim, B.-S.; Cho, J. H. Highly Tunable Charge Transport in Layer-by-Layer Assembled Graphene Transistors. *ACS Nano* **2012**, *6*, 2432−2440.
(35) Englert, J. M.; Dotzer, C.; Yang, G.; Schmid, M.; Papp, C.; Gottfried, J. M.; Steinrück, H.-P.; Spiecker, E.; Hauke, F.; Hirsch, A. Covalent Bulk Functionalization of Graphene. *Nat. Chem.* **2011**, *3*, 279−286.
(36) Rice, J. E.; He, Z. M. Preparation of 4- and 10-Fluorobenzo-[J]Fluoranthene Via Cyclodehydration of Acetals and Cyclopropylcarboxaldehydes. *J. Org. Chem.* **1990**, *55*, 5490−5494.
(37) Acik, M.; Lee, G.; Mattevi, C.; Pirkle, A.; Wallace, R. M.; Chhowalla, M.; Cho, K.; Chabal, Y. The Role of Oxygen During Thermal Reduction of Graphene Oxide Studied by Infrared Absorption Spectroscopy. *J. Phys. Chem. C* **2011**, *115*, 19761−19781.
(38) Krause, B.; Petzold, G.; Pegel, S.; Pötschke, P. Correlation of Carbon Nanotube Dispersability in Aqueous Surfactant Solutions and Polymers. *Carbon* **2009**, *47*, 602−612.
(39) Bagri, A.; Mattevi, C.; Acik, M.; Chabal, Y. J.; Chhowalla, M.; Shenoy, V. B. Structural Evolution During the Reduction of Chemically Derived Graphene Oxide. *Nat. Chem.* **2010**, *2*, 581−587.
(40) Zhang, F.; Jiang, H.; Li, X.; Wu, X.; Li, H. Amine-Functionalized Go as an Active and Reusable Acid−Base Bifunctional Catalyst for One-Pot Cascade Reactions. *ACS Catal.* **2014**, *4*, 394−401.
(41) Wong, C. H. A.; Sofer, Z.; Kubešová, M.; Kučera, J.; Matějková, S.; Pumera, M. Synthetic Routes Contaminate Graphene Materials with a Whole Spectrum of Unanticipated Metallic Elements. *Proc. Natl. Acad. Sci. U. S. A.* **2014**, *111*, 13774−13779.
(42) Wang, L.; Ambrosi, A.; Pumera, M. Metal-Free" Catalytic Oxygen Reduction Reaction on Heteroatom-Doped Graphene Is Caused by Trace Metal Impurities. *Angew. Chem., Int. Ed.* **2013**, *52*, 13818−13821.
(43) Su, C.; Acik, M.; Takai, K.; Lu, J.; Hao, S.-j.; Zheng, Y.; Wu, P.; Bao, Q.; Enoki, T.; Chabal, Y. J.; Ping Loh, K. Probing the Catalytic Activity of Porous Graphene Oxide and the Origin of This Behaviour. *Nat. Commun.* **2012**, *3*, 1298.
(44) Gómez-Navarro, C.; Weitz, R. T.; Bittner, A. M.; Scolari, M.; Mews, A.; Burghard, M.; Kern, K. Electronic Transport Properties of Individual Chemically Reduced Graphene Oxide Sheets. *Nano Lett.* **2007**, *7*, 3499−3503.
(45) Paredes, J. I.; Villar-Rodil, S.; Martínez-Alonso, A.; Tascón, J. M. D. Graphene Oxide Dispersions in Organic Solvents. *Langmuir* **2008**, *24*, 10560−10564.
(46) Zhang, J.; Yang, H.; Shen, G.; Cheng, P.; Zhang, J.; Guo, S. Reduction of Graphene Oxide Vial-Ascorbic Acid. *Chem. Commun.* **2010**, *46*, 1112−1114.
(47) Chen, C.; Cai, W.; Long, M.; Zhou, B.; Wu, Y.; Wu, D.; Feng, Y. Synthesis of Visible-Light Responsive Graphene Oxide/Tio2 Composites with P/N Heterojunction. *ACS Nano* **2010**, *4*, 6425−6432.
(48) Pegel, S.; Pötschke, P.; Petzold, G.; Alig, I.; Dudkin, S. M.; Lellinger, D. Dispersion, Agglomeration, and Network Formation of Multiwalled Carbon Nanotubes in Polycarbonate Melts. *Polymer* **2008**, *49*, 974−984.
(49) Azoubel, S.; Magdassi, S. The Formation of Carbon Nanotube Dispersions by High Pressure Homogenization and Their Rapid Characterization by Analytical Centrifuge. *Carbon* **2010**, *48*, 3346−3352.
(50) Edenharter, A.; Feicht, P.; Diar-Bakerly, B.; Beyer, G.; Breu, J. Superior Flame Retardant by Combining High Aspect Ratio Layered Double Hydroxide and Graphene Oxide. *Polymer* **2016**, *91*, 41−49.
(51) Han, J. T.; Jang, J. I.; Kim, H.; Hwang, J. Y.; Yoo, H. K.; Woo, J. S.; Choi, S.; Kim, H. Y.; Jeong, H. J.; Jeong, S. Y.; Baeg, K.-J.; Cho, K.; Lee, G.-W. Extremely Efficient Liquid Exfoliation and Dispersion of Layered Materials by Unusual Acoustic Cavitation. *Sci. Rep.* **2014**, *4*, 5133.
(52) Lee, J. U.; Lee, W.; Yi, J. W.; Yoon, S. S.; Lee, S. B.; Jung, B. M.; Kim, B. S.; Byun, J. H. Preparation of Highly Stacked Graphene Papers Via Site-Selective Functionalization of Graphene Oxide. *J. Mater. Chem. A* **2013**, *1*, 12893−12899.
(53) Rourke, J. P.; Pandey, P. A.; Moore, J. J.; Bates, M.; Kinloch, I. A.; Young, R. J.; Wilson, N. R. The Real Graphene Oxide Revealed: Stripping the Oxidative Debris from the Graphene-Like Sheets. *Angew. Chem., Int. Ed.* **2011**, *50*, 3173−3177.
(54) Thomas, H. R.; Day, S. P.; Woodruff, W. E.; Vallés, C.; Young, R. J.; Kinloch, I. A.; Morley, G. W.; Hanna, J. V.; Wilson, N. R.; Rourke, J. P. Deoxygenation of Graphene Oxide: Reduction or Cleaning? *Chem. Mater.* **2013**, *25*, 3580−3588.

DOI: 10.1021/acsami.6b07272
ACS Appl. Mater. Interfaces 2016, 8, 21595−21602